



DESIGN & INVESTIGATION OF QUAD PORT CIRCULARLY POLARIZED T-SHAPED MIMO ANTENNA FOR WI-MAX APPLICATIONS

Piyush Kumar Mishra¹, Aditya Kumar Singh*¹, Amrees Pandey¹, J.A. Ansari¹

¹Department of Electronics & Communication, University of Allahabad, Prayagraj, India
ec.piyush21@gmail.com, amrishpandey19@gmail.com, jaansari@radiffmail.com,

*Corresponding author email: aditya08129@gmail.com

Abstract-

In this communication, a compact ($25 \times 25 \times 1.6 \text{ mm}^3$) Ultra-wideband (UWB) with circularly polarized (CP) quad-port and T-shaped radiating elements are demonstrated for the purpose of C-band and particularly for Wi-MAX applications. The UWB phenomenon has (4.36– 6.90) GHz at port-1 with impedance bandwidths of 45.11 %. The 3-dB ARBW achieved 1.3 GHz at the (4.3-5.8) GHz operating band, which indicates the circular polarization aspects at the desired band. The envelope correlation coefficient (ECC) is < 0.08 and isolation in the radiating elements is more than 20 dB, which has justified the applicability of the proposed MIMO design. The value of DG obtained in terms of ports 1-2, 1-3 & 1-4 are 9.989–9.999 dB, 9.978-10 dB & 9.994–9.999 dB respectively and radiation efficiency of more than 90 % is achieved during the entire operating band.

Keywords: MIMO, Radiating Patch, Radiation Efficiency, Diversity Gain, Envelope Correlation Coefficient, TARC.

1. Introduction

Multiple-input-multiple-output (MIMO) techniques is commonly used for the elevated rate of transmission and strong quality of the communications [1]. On the basis of UWB technologies, wireless transmission appliances capable of transmitting become an enormous range of the channel whereas dominate insufficient powers, the significant challenge of the designing antenna devices are to mitigate the mutual coupling in association with radiator of privileged low volumes of the tiny portable appliances [2,3]. MIMO technology incorporates multi-antenna systems at the transmitter as well as the receiver side to develop several un-correlated channels to achieve high data throughput. The compactness of portable wireless devices demanded the requirements of a small configuration of MIMO antenna which may result in degradation in inter-element isolation and overall system diversity performance. Recently, researchers reported several compact size MIMO antennas with sufficient isolation between the antenna ports [4–6]. In authors have proposed a MIMO antenna designed with integrated capabilities WLAN & WIMAX applications in which defected ground structure is used to increase the isolation between the antenna units [7,8]. However, achieving the compact MIMO antenna with reduced mutual coupling with improved diversity performance is still a field of research. Besides, planar MIMO antennas with circular polarization attributes are favored over

linear polarized (LP) antennas in current wireless devices, as CP antennas solve the problems of polarization mismatch and multipath interference. Circularly polarized (CP) antennas are predominantly utilized for Bluetooth, RFID, WLAN, WiMAX, satellite, and radar applications. Circularly polarized MIMO antennas have the advantage of huge spectral ability since these antennas do not obtain the problem of polarization mismatch between the transmitter and receiver. [9-11]. Signal fading is the key concern for UWB system in the multipath environment, It can be fixed by UWB MIMO antenna which provides improved channel capacity, UWB MIMO antenna have issue of mutual coupling between radiating elements. Mutual coupling can be minimized by Defected Ground Structures (DGS). The proposed work for C band on a wavelength of 1530–1565 nm at the range of 4-8 GHz frequency is mostly used for satellite communications, full-time satellite TV networks or raw satellite feeds. The bands available for satellite communications are 3.4 to 4.2 GHz (downlink i.e. space-to-Earth) and 5.925 to 6.725 GHz (uplink i.e. Earth-to-space) [13,14].

This paper demonstrate quad port T-shaped patch MIMO antenna along with defected ground structure & each T-shaped radiators are designed on the top side of the FR-4 substrate having attributes ($\epsilon_r=4.4$, $\tan\delta=0.019$, and thickness of 1.6 mm). Four port MIMO antenna shows Ultra-Wideband (UWB) (4.36– 6.90 GHz) with impedance bandwidth 45,11% from port-1 for the C-band and particularly for WIMAX applications. The proposed design shows increase gain and Ultra-wideband with valuable MIMO characteristics. T-shaped MIMO antenna is designed and simulated by means of electromagnetic tool High Frequency Structure Simulator (HFSS) v13 by AnSoft. This tool utilizes the mathematical formulation of finite element method. Antenna design and evolution of the proposed antenna structure is presented in section II, result and discussion in section III and conclusions in section IV is presented.

2. Antenna Design and Evolution of the Proposed Antenna Structure

The proposed antenna (Ant-3) geometry where in patch side (red color-top view), ground side (orange color-bottom view) and also specifications or dimensions are in millimeter scale (mm) is shown in Fig.1. Ant-1, Ant-2 & Ant-3 (Proposed antenna) is inset geometry (cf. fig. 2) and radiating patch geometry of all the three antennas is same (cf. fig. 2). Ant-1 is introducing by four T-shaped radiating elements placed in front of each other without defected ground structure (DGS) (cf. fig. 2) as parametric variation is executed on the width of the patch in Ant-1 to enhance the bandwidth. Ant-2 is achieved with four parallel circular slot cut (4 mm) in the ground plane by Ant-1 (cf. fig. 2). Proposed Ant-3 is obtained from Ant-2 by incorporating two rectangular slot cut ($18 \times 2 \text{ mm}^2$) in mid-middle-portion (Cross-way) of the ground plane (cf. fig. 1 & 2) so that in Ant-3 is major role of T-shaped radiating patch and DGS (four circular & two rectangular slot) increase the variation of bandwidth, isolation, operating band & overall gain. Antenna structure is designed using FR4 epoxy material ($\epsilon_r=4.4$, $\tan\delta=0.019$, and thickness of 1.6 mm). The performance of antenna as concerns of return loss, Surface current, gain, axial ratio, radiation patterns. Also MIMO characteristics like ECC (envelope correlation coefficient), DG (diversity gain) and TARC (total active reflection coefficient) is analyzed by means of ANSYS HFSS version 13 as discussed later.

The systematic growth of Ant-1, Ant-2 & Ant-3 is presented in inset of Fig. 2 and their $|S_{11}|$, gain (in dBi) and isolation/mutual coupling (in dB) characteristics are presented in Fig. 2, 3, 4 & 5 respectively.

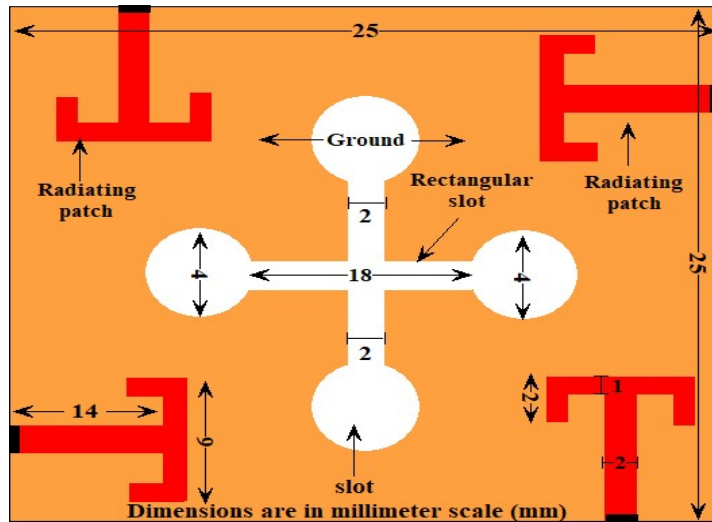


Figure.1 sUpper (red-color) and lower (orange-color) view layout of the proposed antenna

3. Results and Discussion

The proposed antenna is investigated in conditions of return loss, current distribution, envelope correlation coefficient, diversity gain, radiation pattern, radiation efficiency, axial ratio and total active reflection coefficient. Single band (Ant-1, Ant-2, Ant-3) operations have been observed. The table 1 depicts number of operating bands and its operating band frequency, its percentage impedance bandwidth, isolation, resonant frequency of the concerned band, maximum emission point and peak gain. Fig. 2, 3 and 4 represents the variation $|S_{11}|$, isolation (both in dB) & gain (in dBi) with frequency as tabulated in table 1 and also represent that the axial ratio bandwidth (GHz) with Ant 1, Ant 2, Ant 3 as tabulated in table 2 represents the data of Ant-1, Ant-2 & Ant-3 at both ports, i.e. port 1, 2, 3 & 4 for ready reference.

Table 1: Port Characteristics of the ANT-1, ANT-2 & ANT-3 (Proposed)

| Antenna | Port No | Operating band(GHz)/ Impedance BW (in %) | Isolation (dB) | Resonant frequency (GHz) | Reflection Coefficient (dB) | Peak Gain (dBi) |
|---------|---------------------------|--|----------------|--------------------------|-----------------------------|-----------------|
| | Port 1 (S ₁₁) | 3.03-4.95/48.12 | <-21 | 3.9 | -30.7 | -2.6 |
| | Port 2 | 3.06-4.96/47.38 | <-20 | 3.9 | -30.7 | -2.5 |

| | | | | | | |
|-----------------------------|---------------------------|-----------------|------|------|--------|------|
| ANT-1 | (S ₂₂) | | | | | |
| | Port 3 (S ₃₃) | 3.06-4.99/47.39 | <-21 | 3.91 | -29.66 | -2.6 |
| | Port 4 (S ₄₄) | 3.06-4.95/47.25 | <-20 | 3.9 | -29.02 | -2.6 |
| ANT-2 | Port 1 (S ₁₁) | 4.60-6.04/27.06 | <-20 | 5.39 | -18.28 | -0.6 |
| | Port 2 (S ₂₂) | 4.59-6.05/27.49 | <-20 | 5.38 | -18.54 | -0.6 |
| | Port 3 (S ₃₃) | 4.48-6.04/29.65 | <-19 | 5.39 | -18.28 | -0.5 |
| | Port 4 (S ₄₄) | 4.60-6.03/26.93 | <-20 | 5.39 | -18.28 | -0.5 |
| ANT-3 (Proposed) | Port 1 (S ₁₁) | 4.36-6.90/45.11 | <-20 | 5.59 | -27.99 | 2 |
| | Port 2 (S ₂₂) | 4.34-6.90/45.55 | <-21 | 5.59 | -27.58 | 2 |
| | Port 3 (S ₃₃) | 4.35-6.90/45.37 | <-21 | 5.59 | -27.99 | 2 |
| | Port 4 (S ₄₄) | 4.36-6.88/45.11 | <-21 | 5.59 | -26.99 | 2 |

Table2: Comparative Performance Analysis of Antennas with ARB (GHz) & ARBW (GHz)

| Antenna | ARB(GHz)/ARBW(GHz) |
|--------------|---|
| ANT-1 | No usable band (linear polarization) |

| | |
|------------------|---|
| ANT-2 | No usable band (linear polarization) |
| ANT-3 (Proposed) | 4.3-5.8 GHz /1.3 GHz (circular polarization) |

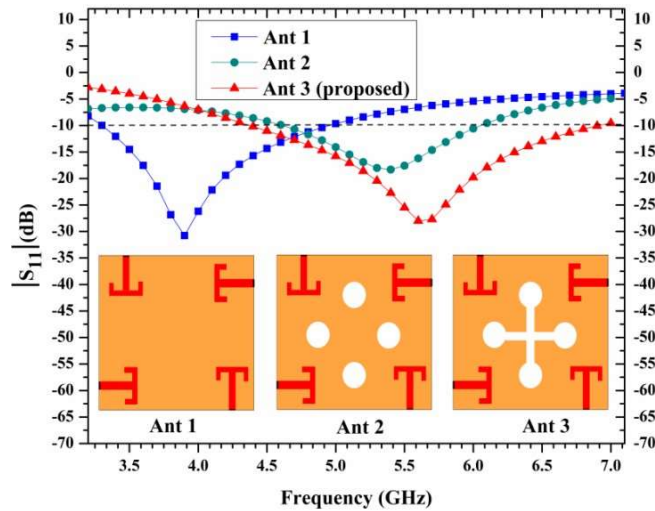


Figure.2 $|S_{11}|$ versus frequency of Ant-1, Ant-2 & Ant-3

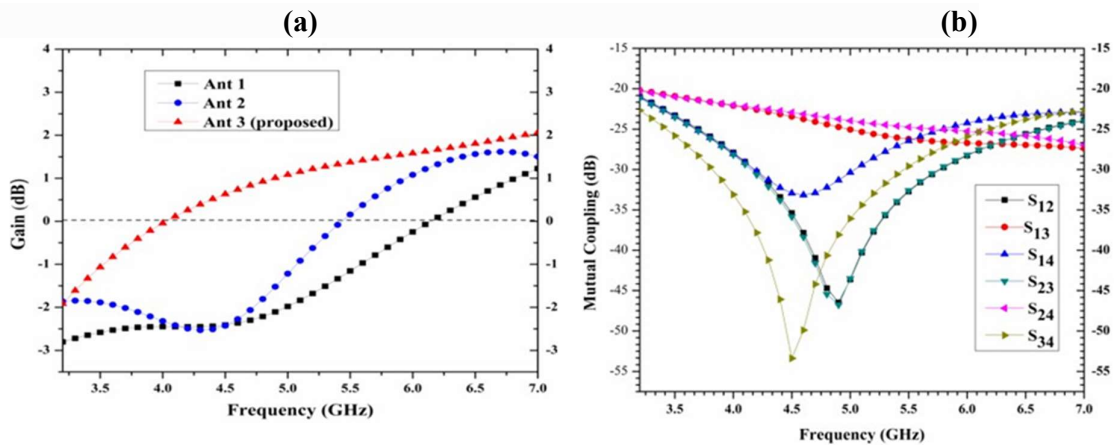


Figure.3 (a) Gain versus frequency of Ant-1, Ant-2 & Ant-3 and (b) Mutual coupling (between the port) of the proposed antenna (Ant-3)

A perusal of table-1 and figs. 2, 3 & 4 clearly shows that operating band and gain characteristics of Ant-1, Ant-2 & Ant-3 are matching at the all ports (port -1, port-2 & port-3) with marginal variation whereas for Ant-1, Ant-2 and Ant-3 the variation of isolation, operating band & overall gain are larger as compared to Ant-3 (proposed). As observed in fig 2, the working

frequency of the T-shaped antenna work as band pass filter which covers the (4.36-6.90 GHz) band and Ultra-wideband having impedance bandwidths increased 45.11% at the port 1 in proposed Ant-3 as compared to Ant 2 but in Ant-1 has favorable impedance bandwidth as compared to Ant-3 but decrease the gain (dBi).

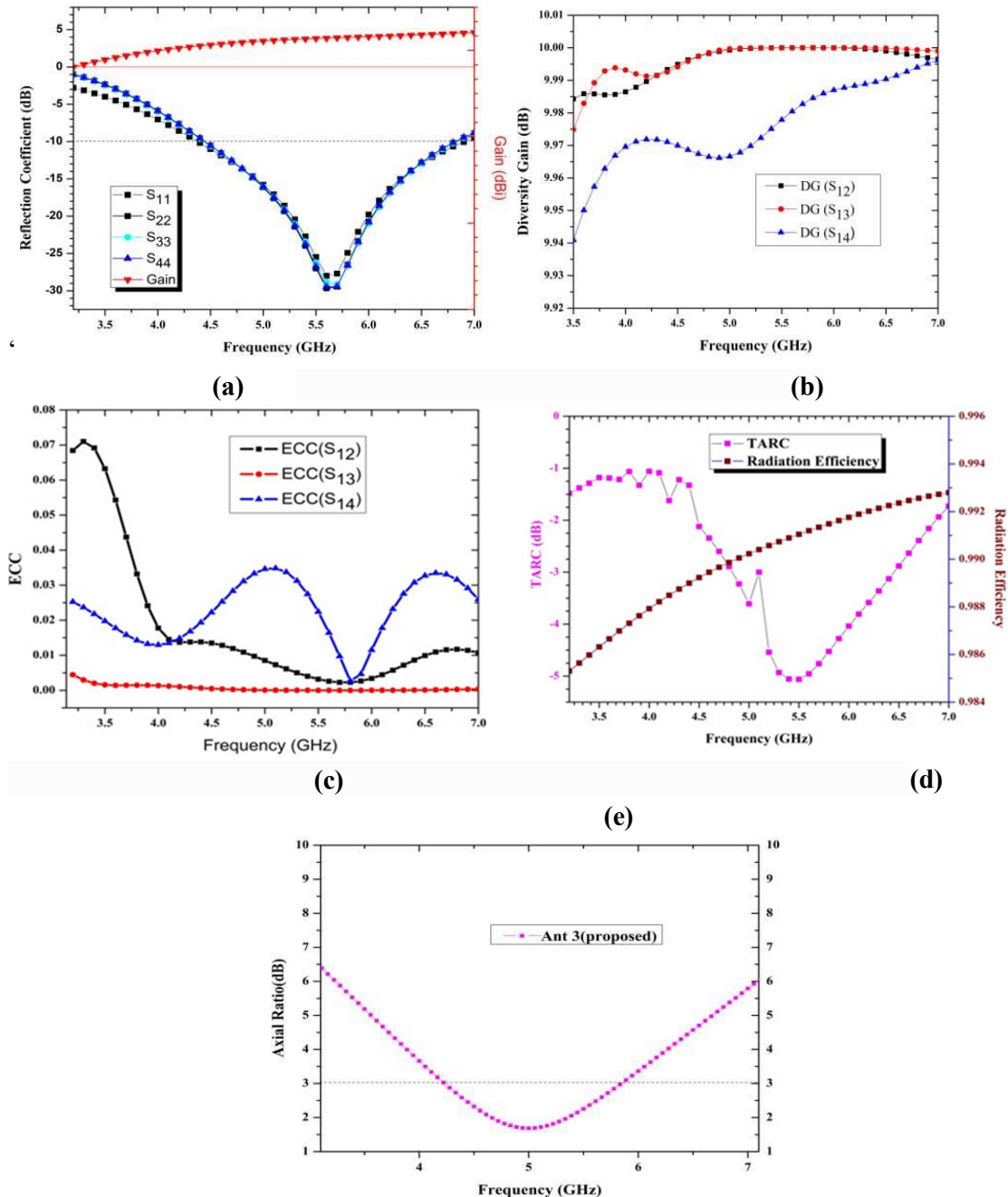


Figure.4 Simulated (a) $|S_{11}|$, $|S_{22}|$, $|S_{33}|$, $|S_{44}|$ gain (b) DG (c) ECC versus frequency plot of the Ant-3(Proposed) (d) TARC & Radiation Efficiency and (e) Axial Ratio (four ports) of Ant-3

ECC is one of the important conduct parameter of MIMO systems, and it is calculated applying

Equation 1, 2, 3 and 4. (cf. fig.4-c) layout of the ECC curve of the proposed antenna over frequency, the values of $ECC < 0.08$ obtained between ports 1-2, ports 1-3 and ports 1-4 value in the range of 0.065464, 0.010116 and 0.025877 respectively at the operating frequency 5.59 GHz. The diversity gain (DG) represents the degradation in transmission power or diversity performance in terms of SNR due to the implementation of the diversity scheme. The DG of a MIMO antenna can be obtained with the help of equation 5 [9,15,16] and for optimum performance, the value of DG should be close to 10 dB. Fig.4(b) shows the value of DG obtained between ports 1-2, ports 1-3 and ports 1-4 value range of 9.989 – 9.999dB , 9.978 - 10 dB & 9.994 – 9.999 dB respectively. Fig.4 (d) illustrates the simulated TARC as well as simulated radiation efficiency versus frequency plot. The radiation efficiency is above 90% for the resonating band of interest. For the efficient transmission of MIMO antenna less than 0 dB TARC value is required and it is calculated using Equation 6. Total active reflection coefficient (TARC) is the key element to better characterize the diversity indices of the four-element antenna system (MIMO) and to justify the effect of radiated electric field phase variation (elevation angle) on return loss of the MIMO antenna which is used to calculate efficiently the bandwidth and the efficiency of the MIMO antennas. For the N-element MIMO system, it is interpreted as the ratio of the square root of the reflected signal strength to the power fed to the antenna. In MIMO system have the b_i and a_i characterize of the reflected power and the incident power fed to the antenna and they are related to each other as $b=[S]a$. The rate of the TARC for the MIMO system can be executed by (6). The isolation value is ≤ -20 dB (cf. fig.3-b) for the observed bandwidth.[17]

$$ECC = \frac{|\iint_{4\pi} F1(\theta,\phi).F2(\theta,\phi)d\Omega|}{\sqrt{\iint_{4\pi} |F1(\theta,\phi)|^2d\Omega \iint_{4\pi} |F2(\theta,\phi)|^2d\Omega}} \quad 1$$

$$ECC_{12} = \frac{|S_{11}S_{12}+S_{21}S_{22}+S_{13}S_{32}+S_{41}S_{42}|^2}{(1-|S_{11}|^2-|S_{12}|^2)(|S_{13}|^2+|S_{14}|^2)} \quad 2$$

$$ECC_{13} = \frac{|S_{11}S_{13}+S_{12}S_{23}+S_{13}S_{33}+S_{14}S_{43}|^2}{(1-|S_{11}|^2-|S_{12}|^2)(|S_{13}|^2+|S_{14}|^2)} \quad 3$$

$$ECC_{14} = \frac{|S_{11}S_{14}+S_{12}S_{24}+S_{13}S_{34}+S_{14}S_{44}|^2}{(1-|S_{11}|^2-|S_{12}|^2)(|S_{13}|^2+|S_{14}|^2)} \quad 4$$

$$\text{Diversity Gain} = 10\sqrt{1 - ECC^2} \quad 5$$

$$\Gamma_a^t = \frac{\sqrt{\sum_{i=1}^N |b_i|^2}}{\sqrt{\sum_{i=1}^N |a_i|^2}} \quad 6$$

From the observation of S_{11} and axial ratio versus frequency plot it can be inferred that as we are moving from antenna 1 to antenna 3 the respective return loss, impedance bandwidth (IBW), and proposed (Ant-3). 3-dB axial ratio bandwidth (ARBW) is getting better (c.f. Figure 4e). Ant-1 and Ant- 2 are linearly polarized while Ant- 3 are circularly polarized. It

can be no axial ratio band ($AR \leq 3$ dB) of Ant-1 and Ant-2 is observed (cf. Table 2) but the proposed Ant-3 is covering a 3dB range 4.36-6.90 GHz, is wide 3 dB axial ratio bandwidth (1.3GHz) is accomplished. Therefore, axial ratio bands indicate that the Ant-3 exhibits circular polarization at port 1, 2, 3 & 4.

At port 1 for the proposed antenna (Ant-3), we observe the current distribution at single frequency i.e. 21.87 GHz as shown in fig 5. The surface current density at 5.59 GHz. is 68.71 A/m is same for the port 1, 2, 3, & 4. That's why here we only show the current distribution for port 1 only. The current strength is high and equally distributed along all over the patch. This asymmetric design can be used for C- band (4-8) GHz applications with quad-ports as suggested. We can say that the proposed Ultra- wideband quad port MIMO antenna can be profitably work as a band pass filter in the frequency range 4.36– 6.90 GHz.

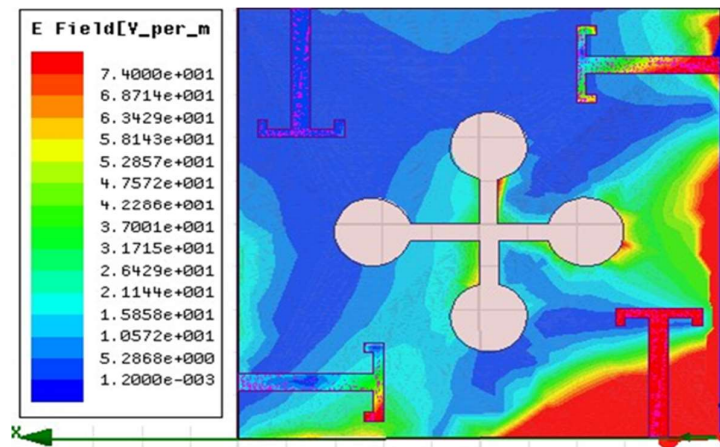


Figure.5 Surface current distribution at port 1 for 21.87GHz

To further confirm the circular polarization attributes of the proposed antenna, simulated synthesized radiation patterns (RHCP and LHCP) plots are presented in Fig. 6. This property of different far-field orientation enables the proposed antenna to accept the same frequency signal at two different polarization, which enhances its signal receiving capability irrespective of polarization orientation. The axial ratio results are shown in Fig. 4 (e). The simulated 3 dB axial ratio bandwidth is closely 1.3 GHz for both the polarized. The proposed quad MIMO antenna have radiation patterns in two dimension for both the E-plane ($\Phi=0^\circ$) & the H-plane ($\Phi=90^\circ$) are put on display in Fig. 6 (a) and (b) respectively. The designed antenna exhibits left-handed circular polarization (LHCP) pattern in the broadside direction at both ports. The principal of E-plane & H-plane have isolation between the LHCP and RHCP motives is greater than 20 dB which presented & the designed of proposed antenna has valuable XPD (cross-polarization discrimination).

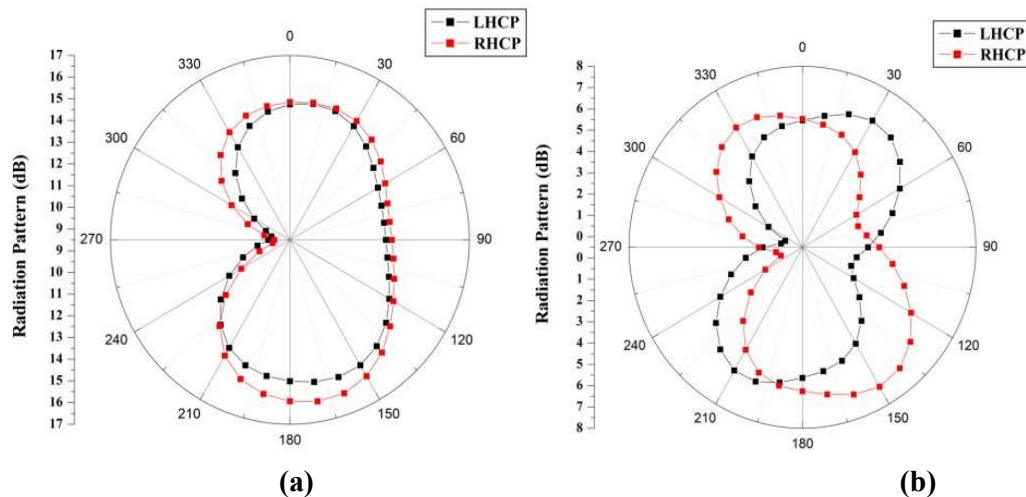


Figure.6 Radiation patterns of the proposed quad port MIMO antenna: Port 1 LHCP and RHCP patterns (a) E plane ($\phi = 0^\circ$) (b) H plane ($\phi = 90^\circ$)

4. Conclusion

In this article, a compact quad port MIMO antenna with T-shaped radiating element is proposed for the C- band (4-8 GHz) and particularly applicable for WiMAX applications. The proposed MIMO antenna has an impedance bandwidth of 45.11% which shows the Ultra-wideband at the desired frequency band (4.36– 6.90 GHz). The proposed antenna provides an axial ratio bandwidth (ARBW) of 1.3 GHz at mentioned operating band which has specify the circularly polarization attributes. The proposed isolation among the radiating elements is less than -20 dB and radiation efficiency is greater than 90% for the whole operating bandwidth within the proposed compact configuration. The diversity performance of the proposed antenna is analyzed and verified in terms of envelope correlation coefficient ($ECC < 0.08$) and total active reflection coefficient ($TARC \leq 0$ dB). The proposed antenna is used for less interference from heavy rain fading & cheaper bandwidth as compared to other bands.

References

- 1) Kumar, S.; Lee, G.H.; Kim, D.H.; Mohyuddin, W.; Choi, H.C.; Kim, K. W. A compact four-port UWB MIMO antenna with connected ground and wide axial ratio bandwidth. International Journal of Microwave and Wireless Technologies, 2020, 20, 1-11.
- 2) Jeeti, C. R.; Nandanavanam, V. R. Trident-shape strip loaded dual band-notched UWB MIMO antenna for portable device applications. AEU - International Journal of Electronics and Communications, 2018, 83, 11-21.
- 3) Wu, Y.; Ding, K.; Zhang, B.; Li, J.; Wu, D.; Wang K. Design of a compact UWB MIMO antenna without decoupling structure. International Journal of Antennas and Propagation, 2018, 26, 1-7.
- 4) Garg, P.; Jain, P. Isolation improvement of MIMO antenna using a novel fower shaped metamaterial absorber at 5.5 GHz WiMAX band. IEEE Transactions on Circuits and

Systems II.2020, 67, 675-679

- 5) Sun, L.; Li, Y.; Zhang, Z.; Feng, Z. Wideband 5G MIMO antenna with integrated orthogonal-mode dual-antenna pairs for metal-rimmed smart phones. *IEEE Trans. Antennas Propag.* 2020, 68, 2494–2503.
- 6) Zhai, G.; Chen, Z. N.; & Qing, X. Mutual coupling reduction of a closely spaced four-element MIMO antenna system using discrete mushrooms. *IEEE Transactions on Microwave Theory and Techniques*, 2016, 64(10), 3060–3067.
- 7) Khan, J.; Sehrai, D.A.; Ali, U. Design of dual band 5G antenna array with SAR analysis for future mobile handsets. *J. Electr. Eng. Technol.* 2019, 14, 809–816.
- 8) Hoang, T. V.; Le, T. T.; Li, Q. Y.; & Park, H. C. Quad-band circularly polarized antenna for 2.4/5.3/5.8-GHz WLAN and 3.5-GHz WiMAX applications. *IEEE Antennas and Wireless Propagation Letters*, . 2016. 15, 1032–1035.
- 9) Dwivedi, A.K.; Sharma, A.; Singh, A.K.; & Singh, V. Circularly Polarized Quad-Port MIMO Dielectric Resonator Antenna with Beam Tilting Feature for Vehicular Communication. *IETE Technical Review* 2021 1-6.
- 10) Srivastava, K.; Mishra, B.; Patel, A. K.; Singh, R. Circularly polarized defected ground stub-matched triple-band microstrip antenna for C- and X-band applications. *MicrowOpt Technol Lett*, 2020, 62, 3301-3309.
- 11) Cheng, Y.; and Liu, H. A novel concentric annular-ring slot dual-band circularly polarized microstrip antenna. *International Journal of Antennas and Propagation*, 2018, 70, 1-8.
- 12) Kumar, S.; Lee, G. H.; Kim, D. H.; Mohyuddin, W.; Choi, H. C.; Kim, K.W. A compact four-port UWB MIMO antenna with connected ground and wide axial ratio bandwidth. *International Journal of Microwave and Wireless Technologies*, 2020, 20(19), 1–11.
- 13) Singh, V.; Mishra, B.; Tripathi, N.P.; Singh, R. A compact quad-band microstrip antenna for S and C-band applications. *Microw Opt Technol Lett.* 2016, 58(6), 1365-1369.
- 14) Bairami, P.; Zavvari, M. Broad band circularly polarized square slot array antenna with improved sequentially rotated feed network for C-band application. *Int J Microw Wirel Technol.* 2017, 9(1), 171- 175.
- 15) Khalid, M.; Iffat, N. S.; Hussain, N.; Rahman, M.; Fawad, Mirjavadi.; Khan S.S.; Amin, M.J. 4-Port MIMO Antenna with Defected Ground Structure for 5G Millimeter Wave Applications. *Electronics* , 2020, 9, 1-13.
- 16) Dwivedi, A. K.; Sharma, A.; Singh, A. K.; & Singh, V. Circularly polarized two port MIMO cylindrical DRA for 5G applications. *International Conference on UK-China*

Emerging Technologies (UCET), 2020, 54, 1–4.

17) Chae, S. H.; Oh, S.; & Park, S.O. Analysis of mutual coupling, correlations, and TARC in WiBro MIMO array antenna. IEEE Antennas and Wireless Propagation Letters, 2007, 6, 122– 125.